UNDRAINED BEARING CAPACITY OF EMBEDDED STRIP FOOTINGS UNDER VERTICAL AND HORIZONTAL LOADS

D. BENMEDDOUR, H. YAHIA-CHERIF, M. MELLAS

Department of Civil and Hydraulic Engineering, University of Biskra, BP 145 Biskra 07000, Algeria

ABSTRACT

This paper is concerned with the undrained bearing capacity of embedded strip footing under inclined loading (i.e. combined vertical and horizontal). A series of numerical computations using the finite-difference code Fast Lagrangian Analysis of Continua (FLAC) was carried out to evaluate the failure envelopes in vertical force – horizontal force (V-H) plane, using both probe and swipe analyses. The adopted approach involves a numerical solution of the equations governing elasto-plastic soils. The soil is modeled by an elasto-plastic model with a Tresca criterion. The results are presented in terms of the failure envelope in vertical and horizontal loading plane.

KEYWORDS: bearing capacity, inclined loads, failure envelope, numerical modeling, embedded foundation.

1 INTRODUCTION

The bearing capacity of foundations has been extensively studied by several methods; these methods may be classified into the following four categories: (1) the limit equilibrium method (e.g., [1-3]); (2) the method of characteristics, (e.g., [4-5]), (3) the limit analysis method, which includes upper bound and lower bound theorems (e.g., [6-8]), and (4) numerical methods that are based on either the finite-element or the finite-difference approaches [9-10].

In practice, the bearing capacity of a strip footing is generally evaluated using the superposition equation proposed by Terzaghi [1]; this equation is valid for a situation where the shallow strip footing is subjected to centered vertical loads, which involves a symmetric failure mechanism.

Exact solution for the undrained vertical bearing capacity for a surface strip footing on idealized plastic material is well established. Expressed in terms of bearing capacity factor $N_c=q_u/c_u$, where q_u is the limiting vertical stress and c_u the representative undrained shear strength, N_c for strip footing is equal to 5.14 (Prandtl [11]). A closed-form exact solution defining ultimate limit states under combined VH loading for a surface foundation on a Tresca material was obtained by Green [12]. However, no exact solution is available for the vertical bearing capacity of an embedded strip.

Undrained vertical bearing capacity of shallowly embedded foundations has been addressed extensively through empirical, analytical and numerical studies for a range of foundation/soil interface condition (e.g., Skempton, [13]; Meyerhof, [14]; Hansen, [15]; Houlsby and Martin, [16]; Salgado et al., [17]; Edwards et al., [18]). However, very little work has addressed inclined bearing capacity of embedded strip footing and no exact solution has been identified. For a strip surface footing under inclined loading, the undrained bearing capacity is calculated as follows:

$$q_u = c_u N_c i_c \tag{1}$$

Where c_u is the undrained shear strength, N_c is the bearing capacity factor and i_c is the load inclination factor. For vertical loading the inclination factor has a value of 1 and the solution is identical to Prandtl's solution. In the literature, there are expressions for the undrained inclination factor, Table 1 summarises the expressions proposed by different authors to evaluate the inclination factor for undrained bearing capacity

Capacity under the interaction of vertical and horizontal loads is conveniently represented by a failure envelope V, H load space. Recently, Gourvenec [19]; Gourvenec and Barnett [20]; Bransby and Randolph [21], investigated the failure surfaces in (H, V, and M) load space through analytical and numerical studies of embedded strip footing. Their results show that the size and shape of failure envelopes defining the undrained capacity of shallow foundations under general loading are dependent on embedment ratio.

In this paper, a series of numerical computations using the finite-difference code FLAC [22] are carried out to determine the shape of the failure envelopes in vertical force – horizontal force (V-H) plane of an emended strip footing on an undrained soil. The numerical results are compared with the available results in the literature

Table1: Expressions of inclination factor.

Author	i_c
Meyerhof [2]	$\left(1-\frac{\alpha^\circ}{90^\circ}\right)^2$
Hansen [4]	$0.5-0.5\sqrt{1-\frac{H}{Bc_u}}$
Vesić [3]	$1-\frac{2H}{Bc_uN_c}$
Green [4]	$0.5+\frac{1}{N_c}\left[\cos^{-1}\left(\frac{H}{Bc_u}\right)+\sqrt{1-\left(\frac{H}{Bc_u}\right)^2}\right]$

2 NUMERICAL MODELING PROCEDURE

In this paper, the finite-difference code FLAC was used to reach the undrained bearing capacity for embedded strip footings under vertical and horizontal loads. The embedment ratio D/B of 0 (surface), 0.25, 0.5 and 1 were considered, where D is the depth of embedment and B is the footing width. In the current modeling study the width B of the footing is 2 m. Because of the absence of loading symmetry, the entire soil domain of width $40B$ and depth $20B$ is considered. The boundary conditions are shown in Figure 1. The base of the model is constrained in all directions. The right and the left vertical sides are constrained in the horizontal direction only.

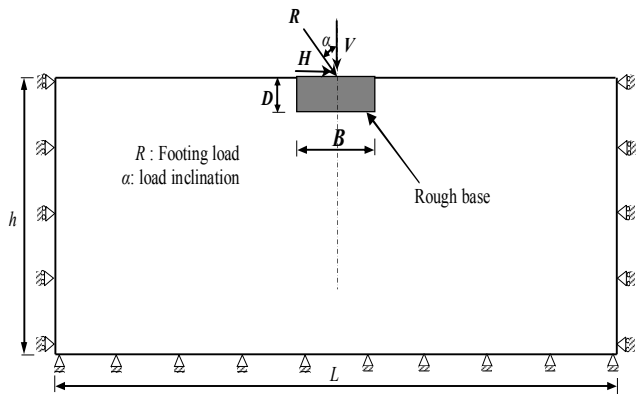

Figure 1: Problem geometry and boundary conditions

The evaluation of the undrained bearing capacity for the embedded strip rigid footing under vertical and horizontal loads is based on subdividing the soil into a number of zones, and specifying equal vertical or horizontal velocities to the zone representing the footing. To simulate the rigid footing, the vertical and horizontal displacements of nodes which discretize the strip footing are constrained in the vertical and horizontal directions.

It is worthwhile noting that refinement of the mesh and the choice of a small velocity does produce slightly better results, and the importance of the mesh size in bearing capacity computations was demonstrated earlier by Frydman and Burd [9]. A series of numerical computations have been carried out to test the influence of the mesh size and the magnitude of the velocity applied at the footing nodes. Figure 2 shows a typical finite-difference mesh used in the analysis of strip footing with embedment ratios D/B=0.5. In all cases, the mesh in the footing neighborhood is refined to capture significant displacement gradients.

The boundary EFGH of the rigid footing is connected to the soil via interface elements defined by Coulomb shear-strength criterion. The soil was modelled as a Tresca material (c_u=20 kPa, υ=0.49, E_u=14 MPa and γ=15 kN/m^3). It should be noted that the values of the elastic parameters had a very small effect on the bearing capacity (Mabrouki et al. [10]).

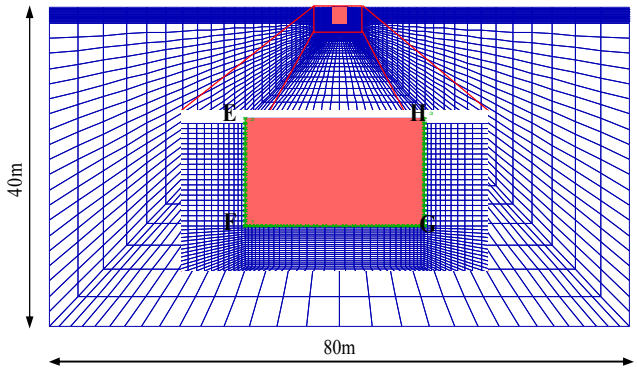

Figure 2: Finite-difference mesh for the case of D/B=0.5.

Both swipe and probe analyses were carried out to identify the (H-V) failure envelope (where H and V are respectively the horizontal and vertical ultimate footing loads). Swipe tests, introduced by Tan [23], are convenient, as a complete failure envelope in a two-dimensional loading plane can be determined in a single test. The swipe tests involve first bringing the foundation to vertical bearing failure, and subsequently applying horizontal velocity while not allowing the footing to move vertically. In the probe analyses, after applying a vertical uniform stresses (smaller than q_u) at the base of the footing; damping of the system is introduced by running several cycles until a steady state of static equilibrium is developed in the soil. Then a controlled horizontal velocity is applied to the nodes situated at the footing. Displacement is increased until failure is reached

3 NUMERICAL RESULTS

3.1 Inclination factor i_c

The load inclination factor defined by normalization of V_{ult} with respect to the limit load for the corresponding vertically loaded footing case $V_{ult,\alpha=0}$. Figure 3(a) presents the inclination factors found in present study for surface footing by probe analyses and those proposed by Meyerhof [2], Hansen [15], Vesić [3] and Green [12]. It shows that i_c decreases as the load inclination α increase. The values of i_c obtained by analytical expressions of Hansen [15], Vesić [3] and Green [12] diverges from the finite difference predictions with increasing load inclination α, where the value of i_c proposed by Green [12] are in excellent agreement with Hansen's expression. The numerical prediction obtained using the finite difference code FLAC is in good agreement with the inclination factor proposed by Meyerhof [2]. Figure 3(b) presents the inclination factors found by the present study using probe analyses for different values of D/B ratio. The figure shows that i_c decreases as the embedment ratio D/B increase.

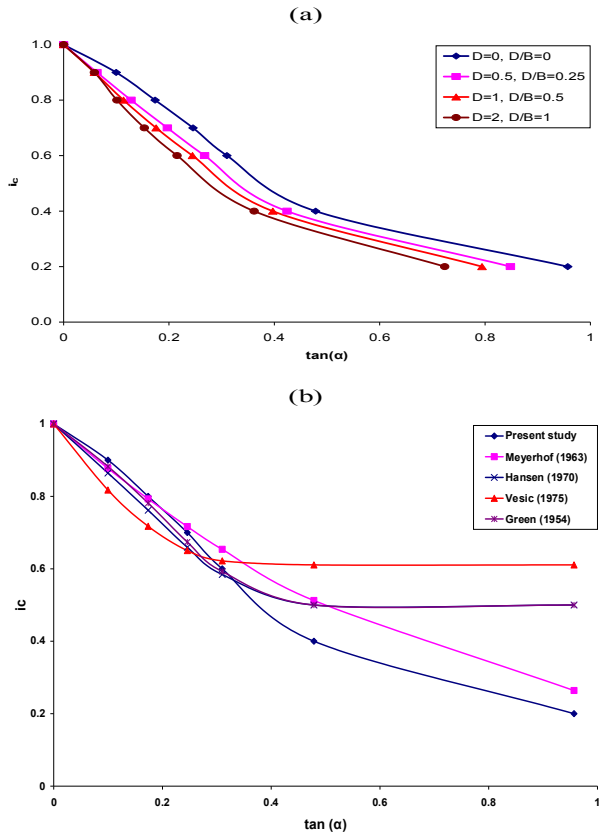

Figure 3: Inclination factor as a function of the load inclination α from probe analyses (a) Comparison with existing expressions (b) Inclination factor as a function of D/B

difference analyses for surface footing (D/B=0) and Hansen's, Vesic's and Green's equations for different load inclinations α. The failure loads define a failure surface in the H–V plane. The study indicates that there is a critical angle of inclination, measured from the vertical direction, above which the ultimate horizontal resistance of the foundation dictates the failure of the foundation. When the inclination angle is more than the critical value, the vertical force does not have any influence on the horizontal capacity of the foundation; the critical angle is predicted to be 17°. The non-dimensional failure envelope predicted by the present numerical analyses is compared in Fig. 4(b), with those of Hansen [15], Vesić [3] and Green [12]. It is noted that for vertical loads less than half the ultimate vertical load V_{ult} the footing fails when the shear strength along the soil–footing interface is fully mobilized, giving sliding failure at the ultimate horizontal failure load of H_{ult}. The Vesic's solution underestimates the normalized loads at low H values and overestimates them at higher horizontal loads.

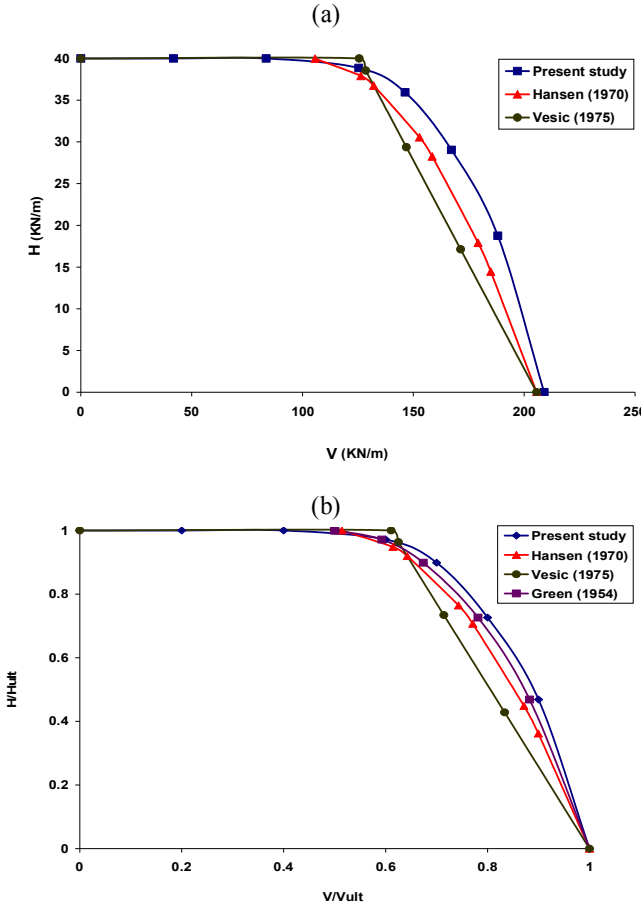

Figure 4: Comparisons of (V-H) failure envelopes for surface footing (D/B=0): (a) comparison with Hansen's, Vesic's and Green's expression. (b) Normalized failure envelopes

3.2 Failure envelope

The dots in Fig. 4(a) represent pairs of failure horizontal (H) and vertical (V) loads obtained from the finite

Figure 5 represents the ultimate limit states normalized by the ultimate limit loads, V/V_{ult} and H/H_{ult}, indicating the shape and relative size of the failure envelopes from probe and swipe analyses for range of D/B ratio of 0 (surface),

0.25, 0.5 and 1. The size of the normalized envelope reduces with increasing embedment ratio. From the figure probe analyses results are in good agreement with the swipe analyses. These results prove that the shape of the failure envelopes are similar and not unique dependent on embedment ratio D/B. Horizontal load governs failure of the foundation for values of V less than about $0.5V/V_{ult}$. A pure sliding mechanism is observed in this region, with $H=H_{ult}$.

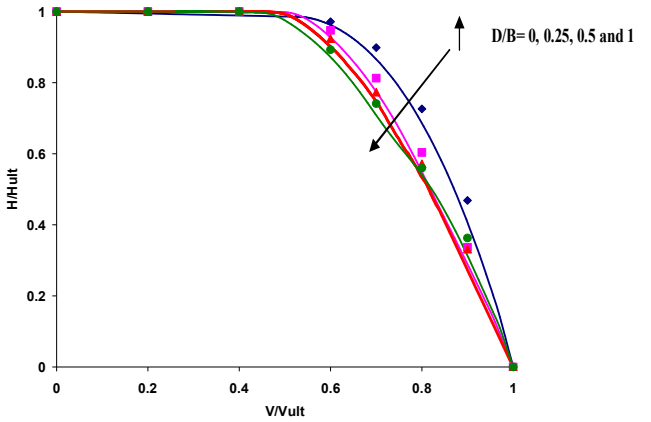

Figure 5: Comparison between the present V–H failure envelope from probe and swipe analyses

3.3 Soil deformation mechanisms

Figure 6(a) shows the contours of maximum shear strain for different load inclination. The plots clearly show the triangular elastic wedge underneath the footing base and demonstrate that there are different mechanisms for different load inclination. Under pure vertical (α=0) loading failure path is symmetrical and similar to the mechanism proposed by Terzaghi [1]. An elastic wedge zone is located immediately below the bottom of the footing pushed the soil in tow symmetrical zone.

However, more α>0, more an asymmetrical double-wedge mechanism prevails, with the footing moving with the soil in the larger wedge zone. The size of the shear zone decreases with increasing values of the load inclination (α). Form figures 6, it is noted that the mechanism of deformation for the embedded foundation is larger than that for the surface foundation. It is worthwhile noting that the value of the maximum magnitude of the displacement vectors varies with the embedment for larger embedment the maximum displacement is higher.

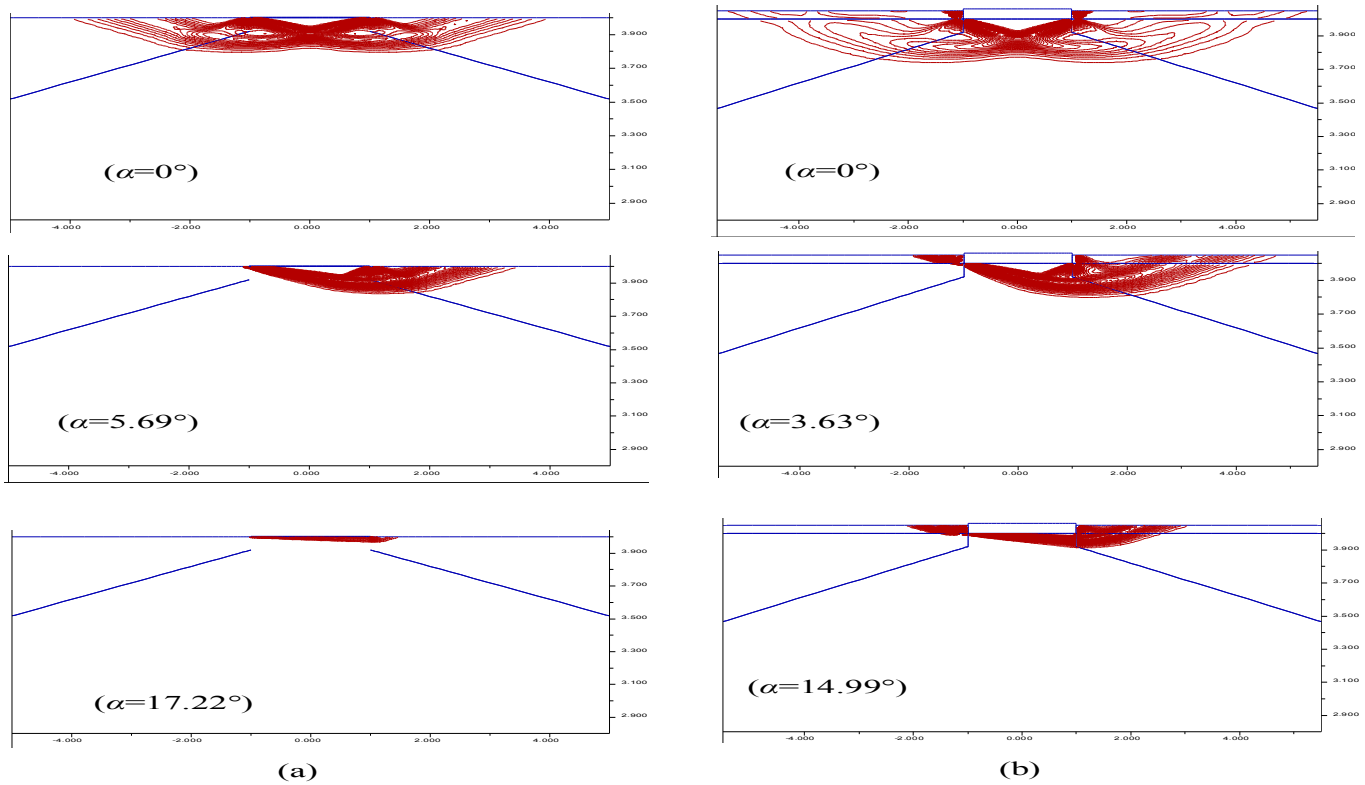

Figure 6: Contours of maximum shear strain for different load inclination

(a) D/B=0, (b) D/B=0.25.

4 CONCLUSIONS

The undrained bearing capacity under inclined loading of embedded strip footing has been investigated. The study proves that the embedment affect the values of inclination factors i_c. The calculations of combined vertical and horizontal loading are summarized in the form of failure envelopes for different values of D/B. Under inclined loading, the shape of the failure envelope is slightly dependent of embedment ratio. The results clarify the reducing of the size of the failure envelope with the increasing of embedment. The contours of maximum shear strain for different load inclination and for different values of D/B proved that the size of the shear zone increases with increasing value of the depth.

REFERENCES

[1] Terzaghi, K. Theoretical soil mechanics. New York: Wiley, 1943.

[2] Meyerhof, G.G. Some recent research on the bearing capacity of foundations. *Can Geotech J* 1963; 1, 16–26.

[3] Vesić A.S. Bearing capacity of shallow foundations. In: Winterkorn HF, Fang HY, editors. Foundation engineering handbook. Van Nostrand Reinhold, 1975.

[4] Hansen J. B. A general formula for bearing capacity. *Dan Geotech Inst* 1961; 11, 38–46.

[5] Sokolovskii, V.V. Statics of soil media (translated from the 1942 Russian edition). London: Butterworths, 1960.

[6] Shield, R.T. Stress and velocity fields in soil mechanics. *Journal of Mathematical Physics* 1954; 33(2), 144–156.

[7] Chen, W.-F. Limit analysis and soil plasticity. *Elsevier*, Amsterdam, 1975.

[8] Michalowski, R.L., and Shi, L. Bearing capacity of footings over two-layer foundation soils. *Journal of Geotechnical Engineering* 1995; 121(5), 421–428.

[9] Frydman, S. & Burd, H.J. Numerical studies of bearing capacity factor N_γ. *J. Geotech. Geoenviron. Engng ASCE* 1997; 123 (1), 20–29.

[10] [Mabrouki, A., Benmeddour, D., Frank, R., Mellas, M. Numerical study of the bearing capacity for two interfering strip footings on sands. *Computers and Geotechnics* 2010; 37, (4), 431–439.

[11] Prandtl L. Uber die Harte Plastischer Korper. Nachr. Ges. Wiss. Goettingen Math. Phys 1920; Kl.,74–85.

[12] Green, A. P. The plastic yielding of metal junctions due to combined shear and pressure. *J Mech. Phys. Solids* 1954; 2 (3), 197–211.

[13] [Skempton, A. W. The bearing capacity of clays. *Proc. Building Research Cong. London*, 1951; 1, 180–189.

[14] Meyerhof, G.G. The bearing capacity of foundations under eccentric and inclined loads. *Proc 3rd Int. Conf. Soil Mech. Found. Engng*, Zurich, 1953; 1 , 440–445.

[15] Hansen J. B. A revised and extended formula for bearing capacity. *Danish Geotech Inst Bull*. 1970; 28, 5–11.

[16] Houlsby, G. T., and Martin, C. M. (2003). Undrained bearing capacity factors for conical footings on clay. *Géotechnique* 2003; 53 (5), 513–520

[17] Salgado, R., Lyamin, A.V., Sloan, S.W., Yu, H.S. Two- and three-dimensional bearing capacity of foundations in clay. *Géotechnique* 2004; 54(5), 297–306.

[18] Edwards, D.H., Zdravkovic, L., Potts, D.M. Depth factors for undrained bearing capacity. *Géotechnique* 2005; 55 (10), 755–758.

[19] Gourvenec, S. Effect of embedment on the undrained capacity of shallow foundations under general loading. *Géotechnique* 2008; 58(3), 177–185.

[20] Gourvenec, S.M. Barnett, S. Undrained failure envelope for skirted foundations under general loading. *Géotechnique* 2011; 61 (3), 263–270.

[21] Bransby, M.F., Randolph, M.F. Combined loading of skirted foundations. *Géotechnique* 1998 48 (5), 637–655.

[22] FLAC – Fast Lagrangian Analysis of Continua, version 5.0. ITASCA Consulting Group, Inc., Minneapolis; 2005.

[23] Tan, F.S.C. Centrifuge and theoretical modelling of conical footings on sand. PhD thesis, University of Cambridge, 1990.

[24] Bransby, M.F., Randolph, M. F. (1999). The effect of embedment depth on the undrained response of skirted foundations to combined loading. *Soils Found* 1999; 39(4), 19 –33.